

Cite this: *Chem. Sci.*, 2025, 16, 4374

All publication charges for this article have been paid for by the Royal Society of Chemistry

Copper(II)-catalyzed enantioselective decarboxylative Mannich reaction coordinated by supramolecular organic amine cages†

Yuanli Zhu,^{‡a} Houting Wang,^{‡a} Rui Liu,^{‡a} Kaihong Liu,^a Xiaodong Hu,^a Jian Huang,^a Cheng Wang,^a Leyi Wang,^a Yan Liu,^{‡b} Guohua Liu^{‡a} and Chunxia Tan^{‡a}

Using supramolecular chiral cages to create a favorable chiral environment can effectively address the limitations of traditional metal asymmetric catalysis in controlling chiral catalytically active centers. However, achieving harmonious interactions among the molecular cage, the metal, and the substrate within the cavity remains a significant challenge. To overcome this, we have designed a pyridinium-modified, chiral-diamine-functionalized cage with a distinct bowl-shaped geometry. This structure features three quaternary ammonium linkers at the base and three chiral cyclohexanediamine units positioned at the rim. Acting as a supramolecular chiral ligand, the coordination of this cage with copper salts forms an optimal chiral environment that enables an efficient decarboxylative Mannich reaction between β -ketoacids and imines, yielding a broad range of chiral β -amino carbonyl compounds. Mechanistic studies and control experiments reveal that the coordinated Cu center is responsible for the substrate grabbing and preorganization within the cavity and the free NH group contributes to the enhanced enantioselectivity through hydrogen bonds, collaboratively enhancing the overall catalytic efficiency.

Received 24th October 2024
Accepted 10th January 2025

DOI: 10.1039/d4sc07212j

rsc.li/chemical-science

Introduction

Since the seminal investigation by Robinson in 1917,¹ the decarboxylative Mannich reaction (DMR) reaction has represented a pivotal advancement in organic synthesis, offering easy access to β -amino carbonyl compounds.^{2–4} This reaction innovatively combines decarboxylation and Mannich-type condensation within a single step, facilitating the C–C bond formation under mild conditions.⁵ In the early stage, the study concerning the DMR focused mainly on the use of β -keto acids and acyclic aldimines to provide racemic β -amino carbonyl compounds in the presence of transition metal catalysts and organic bases,⁶ greatly limiting their application in the synthesis of chiral bioactive molecules and pharmaceutical agents.^{3,6} To overcome these limitations, recent studies have shifted their focus to the use of chiral catalysts.^{3,4,7–10} For example, Ma and co-workers have reported the enantioselective DMR of β -ketoacids and cyclic aldimines in the presence of CuI/(*R,R*)-Ph-Box (copper-

bisoxazoline) as a catalyst (Scheme 1a).^{11,12} Although β -amino carbonyl compounds are produced in high yields, achieving high enantioselectivity is primarily restricted to those conditions utilizing CuI and (*R,R*)-Ph-Box at $-20\text{ }^{\circ}\text{C}$, more stable Cu(II) complexes exhibited inferior enantioselectivity. An alternative established method for synthesizing chiral β -amino carbonyl compounds involves the use of chiral organocatalysts as reported by Ma and co-workers,^{4,13} where the NH groups from saccharide-based amino-thiourea or saccharide-derived axial chiral amine-thiourea are responsible for the enhanced enantioselectivity by mimicking a biomimetic hydrogen bonding system. Recently, covalent organic cages have shown great potential in the construction of enantioselective catalyst systems.^{14,15} Notable examples are the studies by Wang and co-workers, who discovered that the chiral confined space within supramolecular cages can enhance the enantioselective decarboxylative Mannich reaction (DMR) (Scheme 1b).^{9,16} A classic example is the substrate-induced dimerization of tetraamino-bis-thiourea chiral macrocycles, which significantly promotes the enantioselective DMR of cyclic aldimines with β -keto acids.¹⁴ More recently, the same group observed that triazine-containing supramolecular cages could boost the enantioselective DMR of sulfamate-headed cyclic aldimines and malonic acid half-thioesters.⁹ In this study, the triazines in the cages can form lone pair– π interactions with electron-rich substrates in the ground state, which transition to more favorable anion– π interactions in the transition state. Despite the great

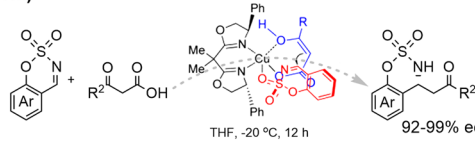
^aShanghai Frontiers Science Center of Biomimetic Catalysis, Joint Laboratory of International Cooperation of Resource Chemistry of Ministry of Education, Shanghai Normal University, Shanghai 200234, China

^bSchool of Chemistry and Chemical Engineering, Frontiers Science Center for Transformative Molecules and State Key Laboratory of Metal Matrix Composites, Shanghai Jiao Tong University, Shanghai 200240, P. R. China

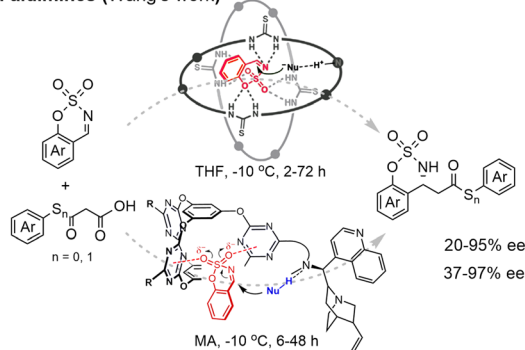
† Electronic supplementary information (ESI) available. See DOI: <https://doi.org/10.1039/d4sc07212j>

‡ These authors contributed equally.

a) Metal-mediated asymmetric DMR of β -ketoacids with aldimines (Ma's work)



b) Hydrogen-bond-directed chiral induction in DMR of β -ketoacids with aldimines (Wang's work)



c) Coordinated copper in supramolecular organic cage for enantioselective DMR reaction (This work)



Scheme 1 Catalytic enantioselective DMRs of β -ketoacids with aldimines. (a) Metal-mediated asymmetric catalysis; (b) supramolecular cage assisted chiral induction catalysis; (c) metal-mediated supramolecular enantioselective transformation (this work).

achievement, these enantioselective DMRs catalyzed by supramolecular cages have predominantly employed aromatic β -keto acids. And the reports on how to achieve high enantioselectivity in the DMR reaction under mild conditions through coordination-induced activation and spatial regulation of the organic cage cavity, similar to enzyme catalysis, remain limited. Consequently, our research interest has been inspired to explore the use of aliphatic β -keto acids in enantioselective DMRs catalyzed by supramolecular cages bearing a more practical grabber (Scheme 1c).

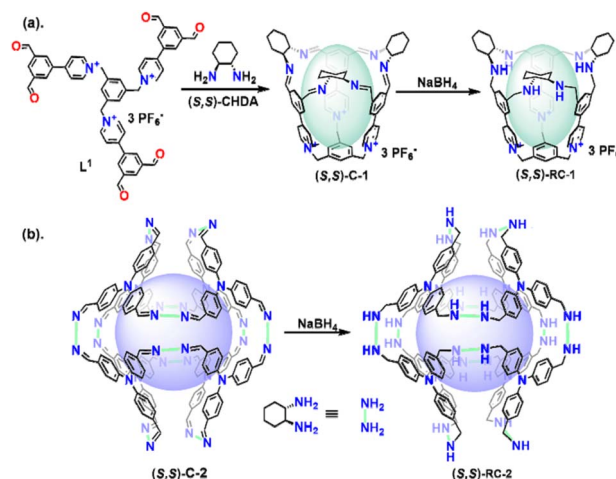
According to the reported mechanism of the DMR, in the case of CuI/(*R,R*)-Ph-Box as a catalyst, the stereocenter was determined by the square-planar coordination of the Cu ion to the enol form of β -ketoacid and the subsequent chelation of the sulfonyl oxygen of the imine to copper.^{8,12} This work indicated that the Cu ion is one of the best grabber candidates for combining cyclic aldimines through coordination bonds. In combination with the mechanism of organocatalysts in the DMR, where the hydrogen bonds between the NH group of the catalyst and O of the imines are responsible for the construction of the stereocenter of the desired β -amino carbonyl compounds,^{4,10} it would be quite possible that the part-coordinated supramolecular cage by Cu species might concurrently balance the benefits of Cu-based catalysts and cages. In this report, we described a Cu part-coordinated cage-mediated

enantioselective decarboxylative Mannich reaction of β -keto acids and cyclic aldimines. As expected, the advantages of the Cu center in capturing substrates and the chiral cages in facilitating stereo-center construction were effectively integrated. Based on HRMS, NMR control experiments, and XPS analysis, a plausible mechanism involving forming coordination bonds between Cu and substrates was proposed.

Results and discussion

Catalyst synthesis

To incorporate the Cu ion into the cage while preserving sufficient free NH groups for hydrogen bond formation with guest molecules, two representative imine-containing cages were selected and synthesized (Scheme 2). The imine cage (*S,S*)/(*R,R*)-C-1, constructed from three chiral 1,2-cyclohexanediamine units and a tricationic hexaaldehyde, was synthesized following the methodology described in Li's work.¹⁷ Treatment of the mixture of hexaaldehyde L¹ and (*S,S*)/(*R,R*)-1,2-cyclohexane diamine ((*S,S*)/(*R,R*)-CHDA) in CH₂Cl₂ at room temperature, afforded the (*S,S*)/(*R,R*)-C-1 in 66% yield as colorless needle-shaped crystals. Similarly, (*S,S*)/(*R,R*)-C-2 was synthesized using the same imine condensation method, employing tris(4-formylphenyl)amine as the aldehyde surrogate.¹⁸ Notably, the reduction of both C-1 and C-2 was achieved in the presence of NaBH₄ (ESI[†]). The evidence to support the formation of RC-1 and RC-2 was derived from the High Resolution Mass Spectrometry (HRMS), NMR and FTIR spectroscopy. Specifically, the peaks at *m/z* 332.2124 and *m/z* 515.8030 for RC-1 and *m/z* = 1810.1681 for RC-2 correspond to [RC-1]³⁺ (calculated: 332.2121) and [RC-1 + Cl]²⁺ (calculated: 515.8026) in HRMS and [RC-2 + 2H]²⁺ (calculated 1810.1838) in MALDI-TOF-MS (Fig. S1[†]). The peaks attributed to the aliphatic -CH- units of the ((*S,S*)/(*R,R*)-CHDA) at 3.28–3.55 ppm shifted to 3.54–3.83 ppm in the ¹H NMR spectrum, which suggests the imine-to-amine transformation. The disappearance of the C=N peak at 1636–1647 cm⁻¹ and the appearance of new peaks at 3132–



Scheme 2 Synthesis of supramolecular amine cages (a) (*S,S*)-RC-1 and (b) (*S,S*)-RC-2.

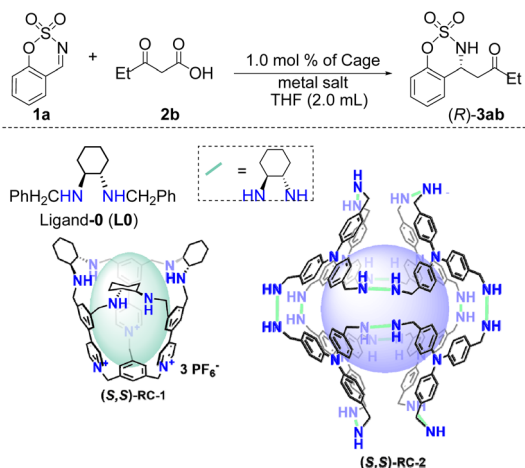


3157 and 1601 cm^{-1} are responsible for the N–H stretching and C–N–H bending vibration (Fig. S2†). The CD spectra for the (*R,R*)/(*S,S*)-**C-1** and (*R,R*)/(*S,S*)-**RC-1** were collected. The CD spectra were similar to those of the corresponding enantiomers, indicating the cotton effects of cages derived from the chiral cyclohexane diamine skeletons.

Screening of reaction conditions

With the desired supramolecular cages in hand, the reaction conditions were optimized to assess their catalytic performance in catalyzing the DMR using **1a** and **2b** as models outlined in Table 1. The model reaction was initially performed using

Table 1 Optimization of the DMR process of **1a** and **2a**^a



| Entry | Catalyst | Time (h) | Yield ^b (%) | ee ^c (%) |
|-------|--|----------|------------------------|---------------------|
| 1 | RC-1 /Cu(OAc) ₂ | 2 | 98 | 96 |
| 2 | RC-1 /Cu(OAc) ₂ ^d | 2 | 98 | 87 |
| 3 | RC-1 /Cu(OAc) ₂ ^e | 2 | 90 | 72 |
| 4 | RC-1 /Cu(OTf) ₂ | 2 | 95 | 94 |
| 5 | RC-1 /Cu(NO ₃) ₂ | 2 | 96 | 92 |
| 6 | RC-1 /CuCl ₂ | 2 | 95 | 94 |
| 7 | RC-1 /CuBr ₂ | 2 | 95 | 96 |
| 8 | RC-1 /Cu ₂ (OH) ₂ SO ₄ | 2 | 83 | 48 |
| 9 | RC-1 /Cu ₂ (OH) ₂ CO ₃ | 2 | 76 | 33 |
| 10 | RC-1 /CuSO ₄ | 2 | 81 | 65 |
| 11 | Cu(OAc) ₂ | 24 | 91 | 0 |
| 12 | RC-1 | 48 | 60 | 0 |
| 13 | C-1 | 48 | 16 | 0 |
| 14 | C-1 /Cu(OAc) ₂ | 2 | 98 | 50 |
| 15 | L0 | 6 | 15 | 3 |
| 16 | L0 /Cu(OAc) ₂ ^f | 6 | 92 | 52 |
| 17 | L0 /Cu(OAc) ₂ ^g | 6 | 90 | 48 |
| 18 | L0 /Cu(OAc) ₂ ^h | 6 | 95 | 51 |
| 19 | RC-2 /Cu(OAc) ₂ | 6 | 96 | 80 |
| 20 | C-2 | 48 | 9 | 0 |
| 21 | RC-2 | 48 | 56 | 0 |
| 22 | C-2 /Cu(OAc) ₂ | 6 | 91 | 18 |

^a Reactions were performed with **1c** (73.2 mg, 0.40 mmol), **2b** (98.4 mg, 0.60 mmol), 1.0 mol% of (*S,S*)-catalysts (cage/Cu = 1/1) in 4.0 mL of THF for 2–48 h at 0 °C. ^b The isolated yield. ^c Determined by HPLC. ^d Molar ratio of cage/Cu is 1/2. ^e Molar ratio of cage/Cu is 1/3. ^f Molar ratio of **L0**/Cu is 3/1. ^g Molar ratio of **L0**/Cu is 1/1. ^h Molar ratio of **L0**/Cu is 1/5.

1.0 mol% of a chiral (*S,S*)-**RC-1**, with variations in the copper salt ratios. The catalytic outcomes revealed that the optimal copper salt-to-cage ratio generally lies around 1 : 1 (entry 1), with deviations from this ratio leading to decreased reaction efficiency and enantioselectivity. For example, in the case of 1 : 2 ratio of **RC-1** to Cu(OAc)₂, **3ab** was isolated in up to 98% yield with 87% ee, slightly inferior to the outcome obtained using 1 : 1 ratio of **RC-1** to Cu(OAc)₂ (97% yield and 94% ee, entry 1 vs. entry 2). However, the enantioselectivity of **3ab** has significantly decreased with the 3 equivalent loading of Cu(OAc)₂ (90% yield, 72% ee, entry 1 vs. entry 3). These may be due to that the NH group has been occupied which has a significant influence on the enantioselectivity of **3ab** (entries 1–3). Cu source screening experiments were further performed, and it showed that the use of other Cu(II) sources as the surrogate of Cu(OAc)₂ resulted in **3ab** in beyond 90% of yields and ee (entries 4–7). However, inferior results were also obtained in the case of the Cu source bearing the OH ligand and SO₄²⁻ in terms of moderate yields and low ee's of **3ab** (entries 8–10). Considering the coordination patterns of divalent copper (Cu(II)) with different electronic configurations and oxidation states,¹⁹ it was proposed that the decreased enantioselectivity during the synthesis of **3ab** can also be affected by the coordinated Cu center. Further screening indicated that either Cu(OAc)₂ or **RC-1** as the catalyst can afford **3ab** in moderate to high yields with racemic form, but the reaction time is significantly prolonged (entries 11 and 12). These results implied that the appropriate proportion of chiral amine cage-based copper catalyst performed exceptionally well in achieving a high activity and ee value, this may originate from that the coordinated Cu(OAc)₂ and part of the NH group in **RC-1** can aid in the preorganization of reactants during the synthesis of **3ab**. To further verify the speculation, and determine the importance of the free NH group in the cage, the subunits of **RC-1** were systematically examined. It showed that only 16% of **3ab** was obtained in the case of **C-1** as a catalyst (entry 13), albeit with a large prolonged reaction time (48 h). The yields and ee could be improved to 98% and 50% with the addition of 1 equivalent of Cu(OAc)₂ (entry 14). In combination with the coordination ability of **C-1** to Cu(OAc)₂, it was suggested that the 50% ee of **3ab** might derive from the substrates' preorganization process within the chiral space of **C-1** because compared to the NH unit in **RC-1**, the hydrogen bonds between the N=C unit and O from the substrate are difficult to form.

To assess the significance of the chiral environment within **RC-1**, its subunits were subsequently analyzed. Using (1*S*,2*S*)-*N,N'*-bis(phenylmethyl)-1,2-cyclohexanediamine (PMCHDA, **L0**), compound **3ab** was isolated in 15% yield and 3% of ee. The addition of Cu(OAc)₂ to **L0** under the same reaction conditions leads to an increased ee value up to 52% while preserving the excellent yields (entries 16–18). Specifically, the Cu(OAc)₂/**L0** (3/1) exhibited a higher reaction rate than the pure Cu(OAc)₂ in the case of which the ee of **3ab** cannot be observed (entry 11 vs. entry 16). These results also suggested that Cu(OAc)₂ in **RC-1** may act as a substrate grabber, likely through coordination bonds between the Cu center and substrates, which leads to preorganization of the substrates and increases reaction activity. Notably, the use of an excess of Cu(OAc)₂ did not affect



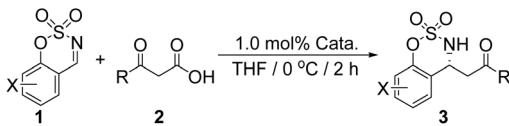
the enantiomeric excess (ee%) of **3ab** (entries 17 and 18). While interesting results were observed with the $\text{Cu}(\text{OAc})_2/\text{L0}$ system, both the reaction rate and enantioselectivity were still slower compared to the outcomes from the **RC-1**/ $\text{Cu}(\text{OAc})_2$ (1/1) (entry 1 vs. entry 16), highlighting the superiority of the chiral microenvironment in the **RC-1** system.

To further demonstrate the hypothesis that the enhanced catalytic performance of **RC-1**/ $\text{Cu}(\text{OAc})_2$ in the enantioselective DMR was primarily attributed to the substrates' preorganization ability induced by the coordinated Cu center and non-coordinated NH group, the octahedral amine cage **RC-2** constructed from twelve chiral 1,2-cyclohexane diamine and eight tertiary aldehydes was synthesized as it features a larger volume and longer linkers. Screening results indicated that the cage **RC-2**/ $\text{Cu}(\text{OAc})_2$ (1/1) exhibited high catalytic performance in the synthesis of **3ab** in terms of yield and ee (96% yield and 80% ee, entry 19). However, due to the unsuitable size match of the confined space for the substrate preorganization in **RC-2**, the ee of **3ab** is inferior to the results obtained using **RC-1**/ $\text{Cu}(\text{OAc})_2$, (entry 1 vs. entry 19). Similarly, the sole **C-2** or **RC-2** without $\text{Cu}(\text{OAc})_2$ resulted in **3ab** in poor to moderate yields as racemic form (entries 20 and 21). When $\text{Cu}(\text{OAc})_2$ is added to **C-2**, the yield of **3ab** can be improved to 91% (entry 22). These results indicated that the combined chiral amine cage and copper salt are crucial in catalytic activity and asymmetric induction, and the substrate preorganization ability was induced by the coordinated Cu center and non-coordinated NH group.

Scope investigation

Having clarified the role of $\text{Cu}(\text{OAc})_2$ and the cage, respective cyclic aldimines **1** and β -keto acids **2** were examined in this DMR asymmetric catalysis process, as shown in Table 2. It was found that **1a** reacted with β -keto acids bearing different steric hindrance and/or rigidity alkyl groups **2a–e** to give **3aa–3ae** in 98–99% yield and 88–96% ee catalyzed by (*S,S*)-**RC-1**/ $\text{Cu}(\text{OAc})_2$ (1/1) (entries 1–5). It was notable that the enantioselectivity gradually decreased as the steric hindrance and/or rigidity of the alkyl chains increased, this result also occurred in the case of *ortho*-, *meta*-, and *para*-substituted cyclic aldimines **1b–e** (Scheme 3). This observation suggested that the confined space of **RC-1** might possess a certain size selectivity due to spatial position matching, indicating that due to the smaller size of alkyl chains they can more easily enter the confined space in **RC-1** for enhanced enantioselectivity. Meanwhile, *ortho*-, *meta*-, and *para*-substituted cyclic aldimines **1a–j** readily reacted with **2b** to afford the final products **3bb–3jb** in 90–99% yields with 72–96% ee (Table 2, entries 6–14). The strong electron-withdrawing substituents exhibit lower reactivity and enantioselectivity (entries 13–14). This may be due to the reduced electron-donating ability of the sulfonic acid oxygen atoms, which are less readily coordinated by Cu^{2+} during the DMR process. However, when cyclic aldimines **1a–f** react with aryl-based phenoxyacetic acid (**2f**) (Table 2, entries 15–20), the final products **3af–3ff** can be obtained in 92–96% yield but the enantioselectivity decreased to 70–82%, due to the larger size of

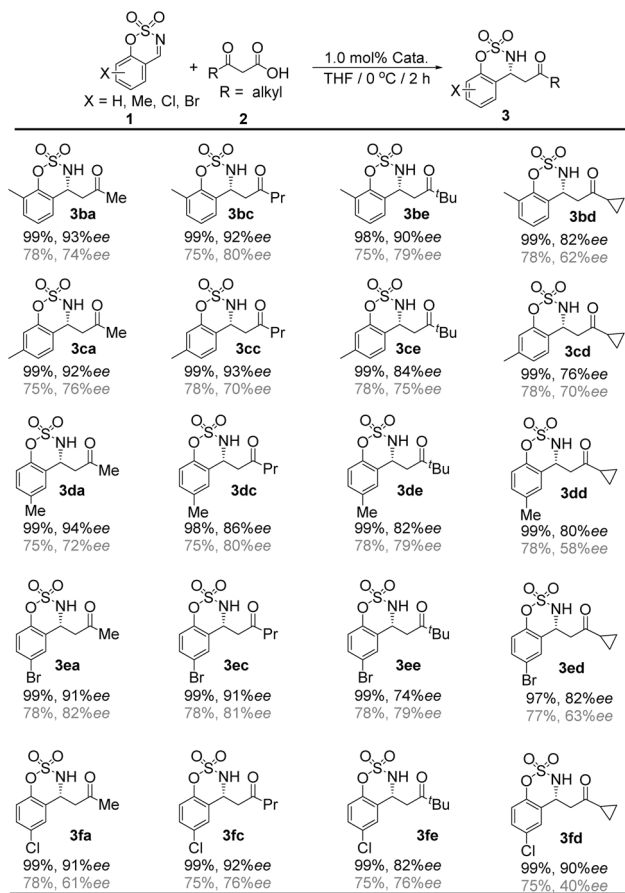
Table 2 DMR of (*S,S*)-**RC-1**/ $\text{Cu}(\text{OAc})_2$ (1/1) and (*S,S*)-**RC-2**/ $\text{Cu}(\text{OAc})_2$ (1/1)^a



| | | (<i>S,S</i>)- RC-1 / Cu^{2+} (1 : 1) | (<i>S,S</i>)- RC-2 / Cu^{2+} (1 : 1) |
|----|---|--|--|
| 1 | 3aa , X, R = H, Me | 98%, 94% ee | 78%, 71% ee |
| 2 | 3ab , X, R = H, Et | 98%, 96% ee | 78%, 78% ee |
| 3 | 3ac , X, R = H, Pr | 98%, 94% ee | 78%, 80% ee |
| 4 | 3ad , X, R = H, ^t Bu | 99%, 94% ee | 78%, 86% ee |
| 5 | 3ae , X, R = H, ⁱ Pr | 99%, 88% ee | 78%, 68% ee |
| 6 | 3bb , X, R = 6-Me, Et | 99%, 92% ee | 78%, 80% ee |
| 7 | 3cb , X, R = 5-Me, Et | 99%, 92% ee | 78%, 78% ee |
| 8 | 3db , X, R = 4-Me, Et | 98%, 90% ee | 78%, 78% ee |
| 9 | 3eb , X, R = 4-Br, Et | 99%, 90% ee | 76%, 81% ee |
| 10 | 3fb , X, R = 4-Cl, Et | 98%, 90% ee | 75%, 74% ee |
| 11 | 3gb , X, R = 4-OMe, Et | 99%, 95% ee | 75%, 76% ee |
| 12 | 3hb , X, R = 4-COOCH ₃ , Et | 95%, 94% ee | 76%, 70% ee |
| 13 | 3ib , X, R = 4-COCH ₃ , Et | 92%, 82% ee | 75%, 66% ee |
| 14 | 3jb , X, R = 4-NO ₂ , Et | 90%, 72% ee | 75%, 50% ee |
| 15 | 3af , X, R = H, Ph | 94%, 88% ee | 79%, 80% ee |
| 16 | 3bf , X, R = 6-Me, Ph | 95%, 80% ee | 76%, 50% ee |
| 17 | 3cf , X, R = 5-Me, Ph | 95%, 76% ee | 72%, 58% ee |
| 18 | 3df , X, R = 4-Me, Ph | 93%, 70% ee | 71%, 56% ee |
| 19 | 3ef , X, R = 4-Br, Ph | 92%, 72% ee | 75%, 62% ee |
| 20 | 3ff , X, R = 4-Cl, Ph | 96%, 76% ee | 76%, 52% ee |

^a Isolated yield, ee is determined by HPLC.





^a Isolated yield, ee is determined by HPLC.
^b catalyzed by (S,S)-RC-1/Cu(OAc)₂ (1/1), in black front.
^c catalyzed by (S,S)-RC-2/Cu(OAc)₂ (1/1), in grey front.

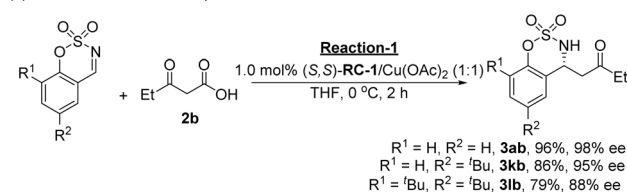
Scheme 3 Substrate scope for the DMR^{a, b, c}.

the aryl-based phenoxyacetic acid, these results further indicate that the spatial position matching of keto acid in the confined cavity in RC-1 plays an important role in the enantioselectivity.

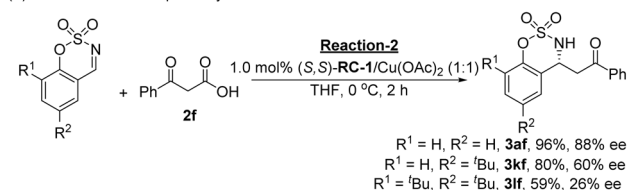
Good yield and enantioselectivity (70–96% ee) were obtained when catalyzed by RC-1/Cu(OAc)₂ (1/1), however when the reaction was catalyzed by RC-2/Cu(OAc)₂ (1/1) the enantioselectivity was down to 50–86% ee, and the enantioselective did not change significantly when the steric hindrance of the keto acid chains increased, this may due to that the inner neutral cavity of RC-2 is rather larger than that of cationic RC-1. This result highlights the significant influence of the electricity and the inner cavity of the container on the catalytic processes of chiral cages.

Further substrate scope investigation focused on the use of bulky substrates. Under the optimized conditions, imines with different steric hindrance (**1g** and **1h**) and 3-oxopentanoic acid (**2b**) could also be well tolerated (Reaction 1 in Scheme 4a), affording corresponding **3gb** and **3hb** in good yields (86% and 79%) and enantioselectivity (95% and 88%), respectively. Considering the excellent yields obtained, it seems that the yield of desired products can be affected by the bulkiness of substrates. To confirm this judgment, the bulky β-keto acid phenoxyacetic acid (**2f**) was then examined (Reaction 2 in

(a) Reactions between 3-oxopentanoic acid and different steric hindrance imine



(b) Reactions between phenoxyacetic acid and different steric hindrance imine



Scheme 4 Size-selective investigation: reaction of (a) 3-oxopentanoic acid or (b) phenoxyacetic acid with imines which have increased spatial hindrance.

Scheme 4b). As expected, the enantioselectivities decreased dramatically from 82% to 26% while yields decreased from 96% to 59% as both the size of the two reactants increased. These results suggest that the present enantioselective DMR might occur within the cage of RC-1.

Mechanistic investigation

To gain mechanistic insight into the present DMR of β-keto acids and cyclic aldimines, a series of characterization studies were performed. According to the design proposal of this work, the semi-coordination of Cu species to RC-1 should be responsible for the high catalytic performance. Therefore, in the beginning, we examined the coordination state of Cu species based on HRMS, ¹HNMR, and XPS analysis. Upon treatment of the equal moles of RC-1 and Cu(OAc)₂ in THF at room temperature, two peaks at 1177.5773 and 588.7887 were observed, which is consistent with the mass of RC-1 plus Cu(OAc)₂, strongly suggesting that only 1 equivalent of Cu(OAc)₂ was coordinated with RC-1 (Fig. S1†). Furthermore, we also observed that the addition of Cu(OAc)₂ to RC-1 induced the H shift of –NH– from 2.12 ppm to 2.39 ppm (see Fig. S4 in the ESI†), which can be rationalized by the coordination of Cu(OAc)₂ to the NH group of RC-1. Because the coordination of HN by Cu decreases the electron density of the nitrogen atom, the proton of RC-1 shifts to the low field in the spectra. The X-ray photoelectron spectroscopy (XPS) investigations further confirmed this coordination since the bonding energy of Cu 2p_{3/2} shifted from 934.30 to 934.40 eV (Fig. 1a and S3†).

Considering that O atoms from either imine or keto acid can coordinate with the Cu center, we next focused on the confirmation of the reaction component which was preferentially captured by the Cu coordinated cage. NMR monitoring experiments indicated that the addition of either keto acid (**2b**) to the solution Cu coordinated cage led to a significant chemical shift in NMR spectra. In contrast, the chemical shift was not observed in the case of the Cu coordinated cage plus imine (**1c**) under the same conditions (Fig. S4 and S5†). These results



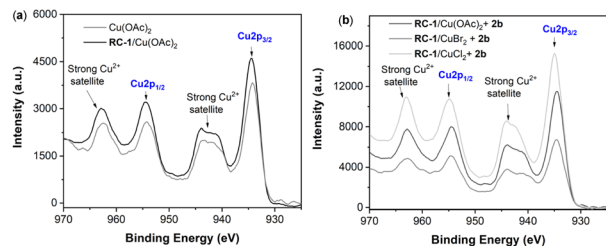
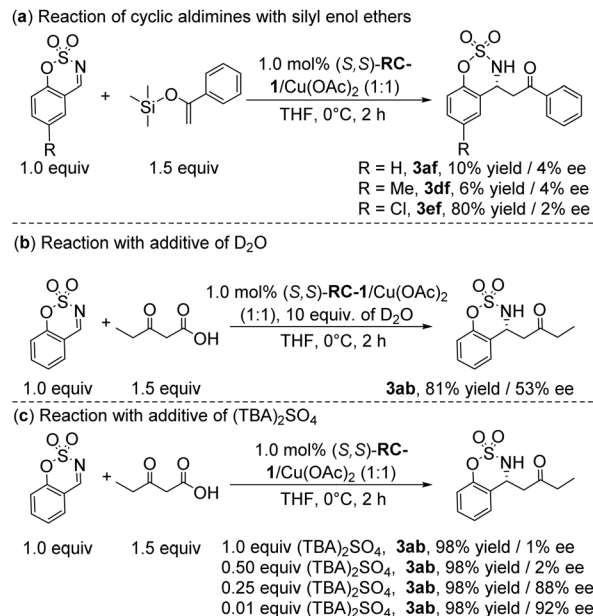


Fig. 1 XPS analysis. (a) Comparison of Cu(OAc)₂ and RC-1/Cu(OAc)₂. (b) XPS of RC-1 with different copper salts after adding the substrate of 3-oxopentanoic acid (2b).

indicated that the keto acid should be preferentially captured by the cage during the catalytic process. This result was further confirmed by investigating the association constant of containers (RC-1-Cu and RC-2-Cu) and the monomer (L0-Cu) toward 7-Me-cyclic aldimines (1c) and keto acid (2b) through UV-vis titration (Fig. S13[†]). The results show that upon gradual addition of imine (1c) or keto acid (2b) into the RC-1-Cu, C-1-Cu cage or L0-Cu solution in THF with a concentration of 1×10^5 mol L⁻¹, the intensity of the absorption band of RC-1-Cu increases at about 250 nm. This result is indicative of the formation of host-guest complexes. In accordance with the linear Benesi-Hildebrand equation, the association constant K_a is estimated to be $(2.74 \pm 0.87) \times 10^4$ M⁻¹, $(5.61 \pm 0.29) \times 10^4$ M⁻¹ and $(1.14 \pm 0.64) \times 10^5$ M⁻¹ for RC-1-Cu, C-1-Cu and L0-Cu bound 1c, respectively, while $(2.55 \pm 0.76) \times 10^4$ M⁻¹, $(1.59 \pm 0.32) \times 10^4$ M⁻¹, and $(9.21 \pm 1.08) \times 10^3$ M⁻¹ for RC-1-Cu, C-1-Cu and L0-Cu bound 2b, respectively. These results show that the binding constant was in the order RC-1-Cu > C-1-Cu > L0-Cu for 2b while L0-Cu > C-1-Cu > RC-1-Cu for 1c. The quite different K_a values combined with the catalysis result of enantioselectivity in the order RC-1-Cu > C-1-Cu > L0-Cu suggested that the DMR reaction was indeed associated with the keto acid being bound in the cavity tightly while the sulfamate may be the heading group inserting within the cavity due to the increased steric hindrance.

To determine the reaction process, a series of control experiments were performed. First, the reaction of 1-phenyl-1-trimethylsiloxyethylene with cyclic aldimines 1a, 1d and 1f was performed. The results show they afforded the final products in 10%, 6%, and 80% yields, respectively, but all of them with no enantioselectivity (Scheme 5a). Silyl enol ethers couldn't be grabbed by the Cu²⁺ in the cage cavity because of the weak coordination ability between the Cu ion and silyl enol, which indicated that grabbing of keto acid by Cu²⁺ is essential for the enantioselective transformation. Then, as deuteration can cause changes in the donor-acceptor distance of the hydrogen bond, and this change leads to an overall alteration in the supramolecular structure,²⁰ the coupling reaction of 1a and 2b was carried out in the presence of D₂O (Scheme 5b). Despite the high yield of 3ab (85%), the enantioselectivity dramatically decreased to 53%. This result may be attributed to alterations in the supramolecular structure, as the geometry of the hydrogen bond is altered upon replacing hydrogen (H) in NH and/or the carboxylic acid group of 2b with deuterium (D). Last, the model

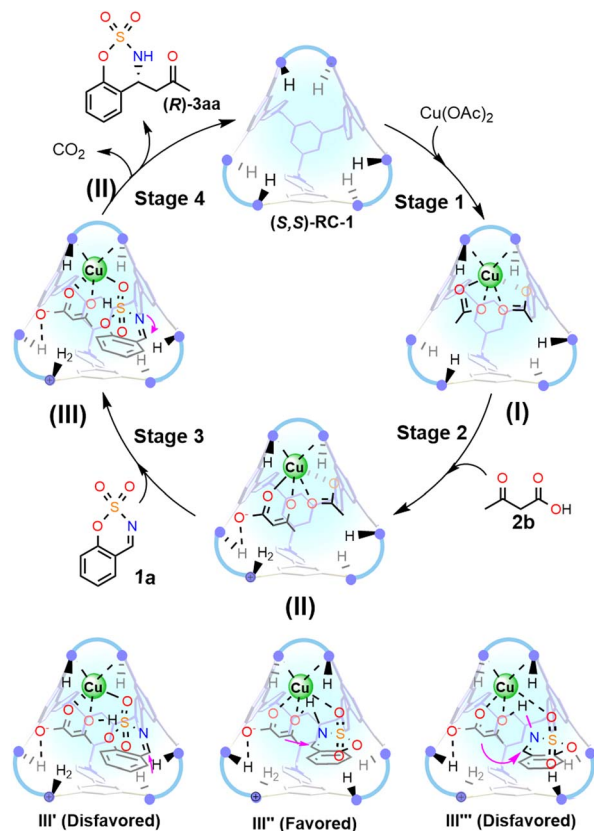


Scheme 5 Control experiment. (a) In the presence of 1.0 equiv. of (TBA)₂SO₄. (b) In the presence of 1.0 equiv. of D₂O. (c) Catalysis between cyclic aldimines with silyl enol ethers.

reaction of 1a and 2b shows that as the concentration of (TBA)₂SO₄ increases the enantioselectivity of 3ab decreases or is even lost (Scheme 5c). Considering the coordination competition between SO₄²⁻ and 2b,¹⁴ this result was suggested that the coordination of imine to Cu of the reaction intermediate is also essential for the construction of the stereocenter of 3ab.

Based on these studies, a plausible cascade mechanism was proposed involving four typical stages, as shown in Scheme 6. In the first stage, the supramolecular chiral ligand (RC-1) initially coordinates with the equivalent of Cu(OAc)₂, forming the part-coordinated Cu-functionalized supramolecular chiral intermediate (I). In the second stage, the substrate β-keto acids (2b) were grabbed and activated by RC-1 coordinated Cu(II) through the ligand exchange process, leading to an enol form chelated intermediate II that facilitates further addition to the imine. Further evidence to support this judgment is from XPS analysis, as compared to intermediate I, the electron binding energy of Cu 2p_{3/2} in the mixture of I and 2b showed a noticeable change from 934.40 eV to 934.60 eV (Fig. 1b and S3[†]). In addition, nearly identical electron binding energies of Cu 2p_{3/2} were observed when using CuCl₂ and CuBr₂ for coordination (934.70, and 934.64 *versus* 934.60, Fig. 2 and S3[†]), suggesting that the counter anions of Cu²⁺ were completely replaced by β-keto acids (2b). This is also consistent with the parallel reactions using CuCl₂ and CuBr₂ in terms of similar catalytic outcomes (entries 6 and 7 in Table 1), thereby demonstrating the dominant role of the supramolecular chiral intermediate (I) during the catalytic process.

In the third stage, the Michael addition occurs as the complexation of the imine (1c) to intermediate II, which leads to the favorable conformation (intermediated III) around the chiral copper active center. Notably, the relatively large steric hindrance would affect the biased face-selectivity with



Scheme 6 Proposed mechanism for the present DMR. The intermediates III and III' originate from (S,S)-RC-1/Cu(OAc)₂, and the intermediates III'' and III''' originate from (R,R)-RC-1/Cu(OAc)₂.

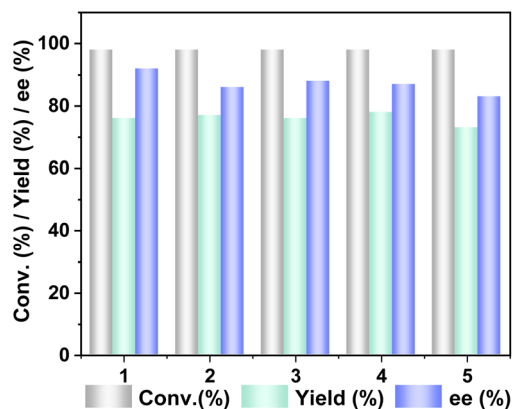


Fig. 2 Reusability of RC-1 using 1a and 2c as substrates.

a favorable conformation as shown in Scheme 6 (intermediates III', III'' and III'''). Furthermore, it was evident that an increase in the steric hindrance of the imine or β-keto acid substrates significantly reduced the enantioselectivity of the reactions (Scheme 3). These results also consisted of the formation of intermediated III, where the enantioselectivity could also be affected by the steric hindrance of the imine substrates.

In the last stage, the decarboxylative process proceeds by releasing chiral products, concomitantly regenerating the active

supramolecular chiral ligand (RC-1), and completing the catalytic cycle. In addition, by comparing the supramolecular chiral ligand (RC-2), it was easily observed that RC-1 exhibits a reaction rate approximately two times faster (Fig. S9†), illustrating that the number of free NH groups close to the Cu center in RC-1 significantly enhanced the reaction efficiency due to the possible assistance of hydrogen bonds, suggesting a collaboration of the NH groups and chiral copper active center. Furthermore, it is worth noting that an alternative reaction pathway, involving the direct addition of imine 1c to 2b before decarboxylation, cannot be ruled out.

The present RC-1 also demonstrated notable stability and high recyclability. RC-1 could be efficiently recovered using a simple hexane extraction and subsequently reused for multiple times. In the enantioselective DMR of 1a and 2b, the RC-1 could be recycled up to five times (Fig. 2), maintaining a consistent conversion and yield while preserving the slightly reduced enantioselectivity from 96% to 83%, thereby affirming the catalyst durability.

In summary, we successfully developed a novel catalytic mode of enantioselective DMR in the presence of part-coordinated amine cages. A series of β-ketoacids and imines can be well tolerated during this catalytic process, yielding a broad range of chiral β-amino carbonyl compounds in excellent yields with high enantioselectivity. Control experiments and mechanistic study indicated that the amine-coordinated Cu center is responsible for grabbing and preorganizing the substrates through the coordination bonds within the confined chiral space, and the free NH group of cages mainly contributed to the enhanced enantioselectivity of the desired β-amino carbonyl compounds through hydrogen bonds. This study not only provided a novel catalytic mode for the construction of chiral products but also highlighted a versatile platform of the covalent organic cage in organic synthesis.

Data availability

The data supporting this article have been included as part of the ESI.†

Author contributions

Y. Z. and H. W. contributed equally. R. L. initiated the concept. Y. Z., H. W., K. L., X. H., J. H., C. W., and L. W. performed the experiments and collected the data. Y. Z., H. W., R. L., G. L. and C. T. analysed the data. R. L., G. L. and C. T. provided the main funding for this work. Y. L., G. L. and C. T. wrote and edited the paper.

Conflicts of interest

There are no conflicts to declare.

Acknowledgements

We are grateful to the China National Natural Science Foundation (22001171, 22001170, and 22071154), the Shanghai



Rising-Star Program (23QA1407200), the Sailing Program (2020YF1435200), the Shanghai STDF (20070502600), and the Shanghai Frontiers Science Center of Biomimetic Catalysis for financial support.

Notes and references

- 1 R. Robinson, *J. Chem. Soc. Trans.*, 1917, **111**, 876–899.
- 2 (a) J. Kaur, A. Kumari, V. K. Bhardwaj and S. S. Chimni, *Adv. Synth. Catal.*, 2017, **359**, 1725–1734; (b) M. Arend, B. Westerman and N. Risch, *Angew. Chem., Int. Ed.*, 1998, **37**, 1044–1070; (c) A. Ting and S. E. Schaus, *Eur. J. Org. Chem.*, 2007, 5797–5815.
- 3 (a) B. N. Lai, J. F. Qiu, H. X. Zhang, J. Nie and J. A. Ma, *Org. Lett.*, 2016, **18**, 520–523; (b) X. Tang, Y. D. Hou, X. F. Tan, J. Nie, C. W. Cheung and J. A. Ma, *ACS Catal.*, 2024, **14**, 9701–9707; (c) X.-Q. Wang, F. F. Feng, J. Nie, F. G. Zhang and J. A. Ma, *Adv. Synth. Catal.*, 2022, **364**, 1908–1912; (d) Z.-L. Wang, *Adv. Synth. Catal.*, 2013, **355**, 2745–2755; (e) S. Nakamura, *Org. Biomol. Chem.*, 2014, **12**, 394–405; (f) D. A. Evans, S. Mito and D. Seidel, *J. Am. Chem. Soc.*, 2007, **129**, 11583–11592; (g) C. Jiang, F. Zhong and Y. Lu, *Beilstein J. Org. Chem.*, 2012, **8**, 1279–1283; (h) F. Zhong, W. Yao, X. Dou and Y. Lu, *Org. Lett.*, 2012, **14**, 4018–4021; (i) J. Zuo, Y.-H. Liao, X.-M. Zhang and W.-C. Yuan, *J. Org. Chem.*, 2012, **77**, 11325–11332; (j) H. W. Moon and D. Y. Kim, *Tetrahedron Lett.*, 2012, **53**, 6569–6572; (k) H.-N. Yuan, S. Wang, J. Nie, W. Meng, Q. Yao and J. A. Ma, *Angew. Chem., Int. Ed.*, 2013, **52**, 3869–3873; (l) Y. K. Kang, H. J. Lee, H. W. Lee and D. Y. Kim, *RSC Adv.*, 2013, **3**, 1332–1335.
- 4 (a) H. N. Yuan, S. Wang, J. Nie, W. Meng, Q. Yao and J. A. Ma, *Angew. Chem., Int. Ed.*, 2013, **52**, 3869–3873; (b) M. Sawa, S. Miyazaki, R. Yonesaki, H. Morimoto and T. Ohshima, *Org. Lett.*, 2018, **20**, 5393–5397; (c) C. W. Suh, C. W. Chang, K. W. Choi, Y. J. Lim and D. Y. Kim, *Tetrahedron Lett.*, 2013, **54**, 3651–3654; (d) M. Tripathi and D. N. J. Dhar, *Heterocycl. Chem.*, 1988, **25**, 1191–1192; (e) B.-H. Zhu, J.-C. Zheng, C.-B. Yu, X.-L. Sun, Y.-G. Zhou, Q. Shen and Y. Tang, *Org. Lett.*, 2010, **12**, 504–507; (f) Y. Luo, A. J. Carnell and H. W. Lam, *Angew. Chem., Int. Ed.*, 2012, **51**, 6762–6766; (g) Y. Luo, H. B. Hepburn, N. Chotsaeng and H. W. Lam, *Angew. Chem., Int. Ed.*, 2012, **51**, 8309–8313; (h) H. Zhang, C. Jiang, J.-P. Tan, H.-L. Hu, Y. Chen, X. Ren, H.-S. Zhang and T. Wang, *ACS Catal.*, 2020, **10**, 5698–5706.
- 5 (a) I. Bagheri, L. Mohammadi, V. Zadsirjan and M. M. Heravi, *ChemistrySelect*, 2021, **6**, 1008–1066; (b) S. Bala, N. Sharma, A. Kajal, S. Kamboj and V. Saini, *Int. J. Med. Chem.*, 2014, **2014**, 191072; (c) T. Guchhait, S. Roy and P. Jena, *Eur. J. Org. Chem.*, 2022, **2022**, e202200578; (d) L. Li, Y. Yao and N. Fu, *Eur. J. Org. Chem.*, 2023, **26**, e202300166; (e) H. Lv, Y. Du, H. Zhang, Y. Zheng, Z. Yan and N. Dong, *ChemistrySelect*, 2023, **8**, e202300173; (f) T. Patra and D. Maiti, *Chem.-Eur. J.*, 2017, **23**, 7382–7401; (g) M. Rahman, A. Mukherjee, I. S. Kovalev, D. S. Kopchuk, G. V. Zyryanov, M. V. Tsurkan, A. Majee, B. C. Ranu, V. N. Charushin, O. N. Chupakhin and S. Santra, *Adv. Synth. Catal.*, 2019, **361**, 2161–2214; (h) A. Varenikov, E. Shapiro and M. Gandelman, *Chem. Rev.*, 2021, **121**, 412–484; (i) Z. Zeng, A. Feceu, N. Sivendran and L. Gooßen, *J. Adv. Synth. Catal.*, 2021, **363**, 2678–2722.
- 6 (a) J. Baudoux, P. Lefebvre, R. Legay, M.-C. Lasne and J. Rouden, *Green Chem.*, 2010, **12**, 252–259; (b) M. Böhm, K. Proksch and R. Mahrwald, *Eur. J. Org. Chem.*, 2013, **2013**, 1046–1049; (c) P. Liu, G. Zhang and P. Sun, *Org. Biomol. Chem.*, 2016, **14**, 10763–10777; (d) P. Qian, Y. Dai, H. Mei, V. A. Soloshonok, J. Han and Y. Pan, *RSC Adv.*, 2015, **5**, 26811–26814; (e) Y. Singjunla, J. Baudoux and J. Rouden, *Eur. J. Org. Chem.*, 2017, **2017**, 3240–3243; (f) T. Xavier, S. Condon, C. Pichon, E. Le Gall and M. Presset, *J. Org. Chem.*, 2021, **86**, 5452–5462; (g) C.-F. Yang, C. Shen, J.-Y. Wang and S.-K. Tian, *Org. Lett.*, 2012, **14**, 3092–3095; (h) F. Zhong, C. Jiang, W. Yao, L.-W. Xu and Y. Lu, *Tetrahedron Lett.*, 2013, **54**, 4333–4336.
- 7 (a) Y. Zheng, H. Y. Xiong, J. Nie, M. Q. Hua and J. A. Ma, *Chem. Commun.*, 2012, **48**, 4308–4310; (b) C. M. Jia, H. X. Zhang, J. Nie and J. A. Ma, *J. Org. Chem.*, 2016, **81**, 8561–8569.
- 8 H.-N. Yuan, S. Li, J. Nie, Y. Zheng and J. A. Ma, *Chem.-Eur. J.*, 2013, **19**, 15856–15860.
- 9 N. Luo, Y. F. Ao, D. X. Wang and Q. Q. Wang, *Angew. Chem., Int. Ed.*, 2021, **60**, 20650–20655.
- 10 H. Guo, Y. F. Ao, D. X. Wang and Q. Q. Wang, *Beilstein J. Org. Chem.*, 2022, **18**, 486–496.
- 11 H. X. Zhang, J. Nie, H. Cai and J. A. Ma, *Org. Lett.*, 2014, **16**, 2542–2545.
- 12 Y. Tang, K. Liu, Y. Wu, S. Zhou, T. Cheng and G. Liu, *Adv. Synth. Catal.*, 2022, **364**, 994–1001.
- 13 Y. J. Liu, J. S. Li, J. Nie and J. A. Ma, *Org. Lett.*, 2018, **20**, 3643–3646.
- 14 (a) R. Saha, B. Mondal and P. S. Mukherjee, *Chem. Rev.*, 2022, **122**, 12244–12307; (b) X. Yang, Z. Ullah, J. F. Stoddart and C. T. Yavuz, *Chem. Rev.*, 2023, **123**, 4602–4634; (c) P. Bhandari and P. S. Mukherjee, *ACS Catal.*, 2023, **13**, 6126–6143; (d) T. Tozawa, J. T. Jones, S. I. Swamy, S. Jiang, D. J. Adams, S. Shakespeare, R. Clowes, D. Bradshaw, T. Hasell, S. Y. Chong, C. Tang, S. Thompson, J. Parker, A. Trewin, J. Bacsá, A. M. Slawin, A. Steiner and A. I. Cooper, *Nat. Mater.*, 2009, **8**, 973–978.
- 15 (a) W. B. Gao, Z. H. Li, T. Y. Tong, X. Qu, H. Dong, L. L. Yang, A. C. H. Sue, Z. Q. Tian and X. Y. Cao, *J. Am. Chem. Soc.*, 2023, **145**, 17795–17804; (b) Y. J. Du, J. H. Zhou, L. X. Tan, S. H. Liu, K. Zhao, Z. M. Gao and J. K. Sun, *ACS Appl. Nano Mater.*, 2022, **5**, 7974–7982; (c) C. García-Simón, R. Gramage-Doria, S. Raoufmoghaddam, T. Parella, M. Costas, X. Ribas and J. N. Reek, *J. Am. Chem. Soc.*, 2015, **137**, 2680–2687; (d) Y. Wang, Y. B. Sun, P. C. Shi, M. M. Sartin, X. J. Lin, P. Zhang, H. X. Fang, P. X. Peng, Z. Q. Tian and X. Y. Cao, *Chem. Sci.*, 2019, **10**, 8076–8082; (e) N. Xu, K. Z. Su, E. S. M. El-Sayed, Z. F. Ju and D. Q. Yuan, *Chem. Sci.*, 2022, **13**, 3582–3588; (f) D. W. Zhang, J. P. Dutasta, V. Dufaud, L. Guy and A. Martinez, *ACS Catal.*, 2017, **7**, 7340–7345; (g) K. Wang, X. Tang, B. A. Anjali, J. Dong, J. Jiang, Y. Liu and



- Y. Cui, *J. Am. Chem. Soc.*, 2024, **146**, 6638–6651; (h) J. K. Sun, W. W. Zhan, T. Akita and Q. Xu, *J. Am. Chem. Soc.*, 2015, **137**, 7063–7066; (i) Y. L. Lu, Y. H. Qin, S.-P. Zheng, J. Ruan, Y.-H. Huang, X. D. Zhang, C. H. Liu, P. Hu, H. S. Xu and C. Y. Su, *ACS Catal.*, 2024, **14**, 94–103; (j) C. Zhao, Q. F. Sun, W. M. Hart-Cooper, A. G. Dipasquale, F. D. Toste, R. G. Bergman and K. N. Raymond, *J. Am. Chem. Soc.*, 2013, **135**, 18802–18805.
- 16 H. Guo, L. W. Zhang, H. Zhou, W. Meng, Y. F. Ao, D. X. Wang and Q. Q. Wang, *Angew. Chem., Int. Ed.*, 2020, **59**, 2623–2627.
- 17 Y. Lei, Q. Chen, P. Liu, L. Wang, H. Wang, B. Li, X. Lu, Z. Chen, Y. Pan, F. Huang and H. Li, *Angew. Chem., Int. Ed.*, 2021, **60**, 4705–4711.
- 18 K. E. Jelfs, X. Wu, M. Schmidtman, J. T. A. Jones, J. E. Warren, D. J. Adams and A. I. Cooper, *Angew. Chem., Int. Ed.*, 2011, **50**, 10653–10656.
- 19 (a) K. D. Karlin and J. Zubieta, *Copper Coordination Chemistry: Biochemical and Inorganic Perspectives*, Academic Press, 1983; (b) M. S. Sigman and E. N. Jacobsen, *Angew. Chem., Int. Ed.*, 1998, **37**, 3000–3010; (c) S. Mun and C. Kim, *ACS Catal.*, 2018, **8**, 9351–9362.
- 20 (a) C. N. Ramachandra, *J. Chem. Soc., Faraday Trans. 1*, 1975, **71**, 980–983; (b) C. Shi, X. Zhang, C.-H. Yu, Y.-F. Yao and W. Zhang, *Nat. Commun.*, 2018, **9**, 481–489.

